Hydrogen enrichment effects in premixed Methane/Air flames

D. Cecere, E. Giacomazzi, F.R. Picchia, N.M. Arcidiacono
donato.cecere@enea.it
Process and Enrgy Systems Engineering Laboratory, Rome, Italy.

Abstract

Nowadays, in the context of CO2 reduction and gas turbine fuel flexibility, the interest in acquiring know-how on lean Hydrogen Enriched Natural Gas (HENG) is growing. This article provides a detailed analysis of a turbulent (Re_{jet}=2476, Re_t=236) lean (Φ=0.7) CH_4/H_2-air premixed slot flames (unconfined and at atmospheric pressure) highlighting the effects of two different hydrogen contents in the inlet mixture (20% and 50% by volume). The data were generated and collected setting up a three-dimensional numerical experiment performed through the Direct Numerical Simulation (DNS) approach and using high-performance computing. Finite difference schemes were adopted to solve the compressible Navier-Stokes equations in space (compact sixth-order in staggered formulation) and time (third-order Runge-Kutta). Accurate molecular transport properties and the Soret effect were also taken into account. A detailed skeletal chemical mechanism for methane-air combustion, consisting of 17 transported species and 73 elementary reactions, was used. The analysis reports average and rms fluctuation of velocity components, temperature and main chemical species mass fractions. New scientific insight is delivered by analysing the probability density functions of several quantities: curvature, shape factor, alignment between vorticity vector and flame surface normal, displacement speed and its components. Correlations between the flame thickness and the progress variable and curvature are also investigated, as well as correlation between strain rates and curvature, and equivalence ratio and curvature. An expression of displacement speed, with diffusion terms taking into account differential diffusion of progress variable species components is derived. The effect of thermal diffusion is also considered. The effects of differential diffusion of several species on the local equivalence ratio are quantified: the maximum variation from the nominal inlet value is $\sim$ 9% and it is due to H2 and O2 .
The addition of Hydrogen reduces the displacement speed at negative curvatures in a range that depends on the local progress variable value, with a maximum variation of -33% between the two flames. The database will also be helpful to validate subgrid models for Large Eddy Simulation.

Test case definition

The test case defined for this study consists in an unconfined premixed slot-burner flame at atmospheric pressure. A slot-burner Bunsen configuration is especially interesting due to the presence of a mean shear in the flow. The configuration is similar to that of the experimental device already analysed in [1] but with smaller dimensions (h=1.2mm vs 25.4mm of slot width in the experimental setup) and higher bulk velocities (100m/s) compared to experiment (3 to 12m/s) to artificially decrease the hydrodynamic DNS times. It consists of a central slot-jet of premixed reactants surrounded on both longer sides by two coflowing jets. The central slot-duct is 1.2 mm wide (h) and 4 mm long; its two walls have a thickness h_w =0.18 mm and are assumed adiabatic in the simulation.

The central jet is a lean (equivalence ratio Φ=0.7) mixture of methane, hydrogen and air with fuel molar fractional distribution of 20% H_2 and 80% CH_4 for the flame A, and of 50% H_2 and 50% CH_4 for the flame B. Mixture temperature is 600 K for flame A, and 588 K form flame B: the latter lower temperature was chosen to achieve the same kinematic viscosity and Reynolds number for the central reactive jet in the two simulations. The surrounding jets have the composition and temperature of the combustion products of the laminar freely propagating flame associated to the central jet mixture. The unstrained laminar flame properties at these conditions computed using Chemkin are summarized in Table 1.

Case	Φ	n_{H_2}	T_u	T_b	S_L^{nS}	δ_L^{nS}	S_L^S	δ_L^S	δ_D^S
A	0.7	0.2	600	2072	1.03	0.368	1.01	0.378	0.1329
B	0.7	0.5	588	2084	1.37	0.314	1.34	0.315	0.1096

Table 1. Laminar flames characteristics (A-B). The superscripts nS and S in the laminar flame speed and flame front thickness, respectively stand for “no Soret” and “Soret” effect not included and included in the laminar flame calculation.

In this table, Φ represents the multi-component equivalence ratio of the reactant jet mixture, $\Phi=[(X_{H2}+X_{CH4})/X_{O2}]/[(X_{H2}+X_{CH4})/X_{O2}]_{stoich}$, T_u is the unburnt gas temperature, T_b the burnt gas temperature, S_L represents the unstrained laminar flame speed and $\delta_{th}=(T_b-T_u)/|\partial T/\partial x|_{max}$ is the flame front thermal thickness based on the maximum temperature gradient. The central jet has a velocity of 100 m/s (imposed as a mean plug-flow at the inlet of the 4 mm long central duct). Homogeneous isotropic turbulence is artificially generated at the inlet of the central duct by forcing a turbulent spatial correlation scale in the streamwise direction $\delta_{z,in}$=0.4 mm and a streamwise velocity fluctuation u'_z=12 m/s used as inputs to the Klein’s procedure. The surrounding flows have a velocity of 25 m/s (imposed as a mean plug-flow) and no turbulence is forced. The actual jet Reynolds number based on the centerline streamwise velocity peak at the central duct exit and its width h is $Re_{jet} = U_o h/\nu$=2476. Other parameters characterizing the present lean premixed turbulent flame are reported in Table 3.

Jet exit velocity peak, U_0 [$\mathrm{m\,s^{-1}}$]	110
Jet exit velocity fluctuation, u' [$\mathrm{m\,s^{-1}}$]	12
Jet exit turbulent length scale, L_t [mm]	1.05
Jet Reynolds number, $Re_{jet} = U_0 h/\nu$	2476
Turbulent Reynolds number, $Re_t = u' L_t/\nu$	236
Kolmogorov lenght scale, η_K [μm]	17.42
Turbulent/chemical speed ratio, u'/S_L	11.88 (8.95)
Turbulent/chemical length scale ratio, L_t/δ_L	2.78 (3.22)
Damkohler number, $S_L L_t/u'\delta_L$	0.238 (0.371)
Karlovitz number, $(\delta_L/\eta_K)^2$	471 (329)

Table 2. Actual turbulent combustion parameters characterizing the simulated CH4 /H2-Air lean premixed flames (flame B in parentheses). The turbulent velocity fluctuation and the integral length scale were evaluated at the center of the exit of the central slot-duct. The laminar flame speed and the flame front thickness including the Soret effect were assumed as combustion parameters. The kinematic viscosity used in the calculation of the central jet Reynolds number is that of the inlet CH_4−H_2/Air A mixture, $\nu = 5.327 \cdot 10^{-5} m^2 s^{-1}$. It is observed that sometimes the Karlovitz number is estimated using the diffusive thickness: with this definition Ka=58 for flame A, and Ka=40 for flame B.

These parameters locate the present flames in the Thin Reaction Zone of the combustion diagram. The computational domain is composed of four structured blocks. The domain size in the streamwise (z), crosswise (y) and spanwise (x) directions is $L_x \times L_y \times L_z$ = 24h×15h×2.5h, h being the slot width (h = 1.2 mm). The grid is uniform only in the x spanwise direction (Δx = 20 μm), it is refined in the y and z direction near the inlet duct walls and coarsened (up to $\Delta y \sim 250$ μm) only in the y direction far from the central jet at the surrounding (y > 0.015 m) where non reflecting boundary conditions are applied and fluctuations are small. The domain is almost identical and the resolution is the same of the work of Richardson et al. [2] and Sankaran et al. [3]. The DNS was run at atmospheric pressure using a 17 species and 73 elementary reactions kinetic mechanism. Periodic boundary conditions were applied in the crosswise direction, while improved staggered non-reflecting inflow and outflow boundary conditions (NSCBC) were adopted at the edges of the computational domain in the y and z directions. The simulation was performed using the HeaRT code, which solves the fully compressible reactive Navier-Stokes equations with the fully explicit third-order time accurate TVD Runge-Kutta scheme of Shu and Osher and a sixth-order compact staggered spatial scheme for non-uniform grid.

Differential diffusivity effect on local equivalence ratio

In order to investigate the effect on local mixture equivalence ratio of differential and thermal diffusion associated with light species as H_2 and H, the local equivalence ratio Φ, is shown for both flames in Fig. 1 as a function of the

normalized curvature at different values of the progress variable.

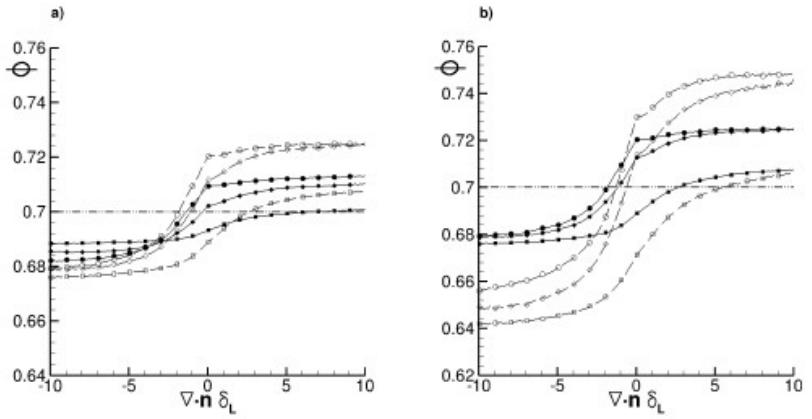

Figure 1. Equivalence ratio at different levels of the progress variable c as a function of the normalized curvature: (circle) c = 0.7, (diamond) c = 0.6, (square) c = 0.4, (Dash dot dot line) nominal flame equivalence ratio Φ. (a) Flame A: (solid line) without Soret effect, (dashed line) with Soret effect. (b) Flame A and B with Soret effect: (solid line) flame A, (dashed line) flame B.

The equivalence ratio Φ is positively correlated with curvature at all progress variable iso-surfaces; the strongest variation is seen in the reaction zone (c∼0.7). This positive correlation can be explained by considering that H_2 is preferentially focused into areas with positive curvature and defocused from areas of negative curvature. The further influence of thermal diffusion is that of enhancing the positive correlation with curvature since it promotes diffusion of light molecules towards high temperature regions. In fact, the maximum equivalence ratio variation is ∼3.7% for flame A and ∼9% for flame B when thermal diffusion effects are considered in the simulation (∼2.6% for flame A when only differential diffusion effect is considered). In order to quantify differential diffusion effects in the two flames, the general method of Sutherland [4] is adopted, and the contribution of major species (H_2, O_2, H, CH_4) differential diffusion term ki to the local variation of mixture fraction, is calculated as:

$$k_i = \nabla \cdot \boldsymbol{j}_i^c, \quad \boldsymbol{j}_i^c = \gamma_i W_i \nabla \cdot [\frac{\rho}{W_{Mix}}(D_i - D)\nabla X_i]$$

where $\gamma_i = \Sigma\, \delta e\, \alpha_{e,i}$, $e=1...N_e$, δ_e are the elemental mass fraction weights of Bilgers's mixture fraction, N_e the number of element e defining the mixture fraction, $\alpha_{e,i}$ is the number of atoms of element e in species i, D the diffusivity of the mixture fraction, D_i the species mass diffusivity. In the enriched flame, the k_{H2} term presents a strongly positive correlation with curvature, and despite the bigger counteracting effect of k_H , it is responsible for the bigger increase of equivalence ratio at positive curvatures of flame B.

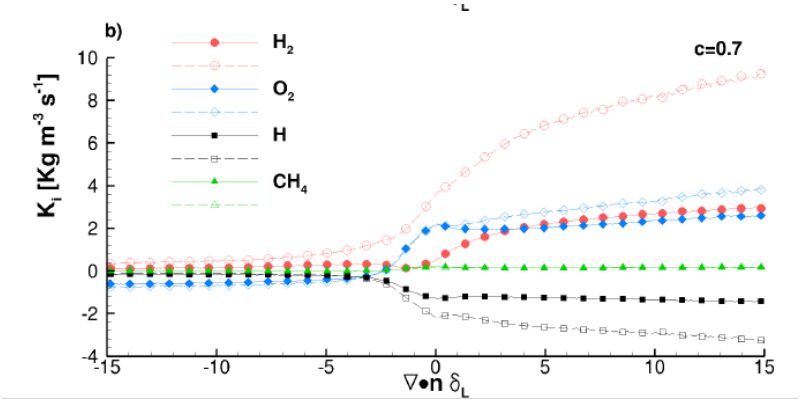

Figure 2. Species differential diffusion source index k_i at c=0.7 level of the progress variable as a function of the normalized curvature for flame A (solid line) and B (dashed line).

Displacement speed versus curvature

Figures 3 shows the mean (averaged on intervals of curvature) density weighted displacement speed S^*_d/S_L and its components plotted against the normalized curvature $\nabla\cdot\mathbf{n}\delta_L$ at a representative values of reaction progress variable (c = 0.8) for flame A with and without Soret effect and for flame B. The data shown in Fig. 3 presents a scatter at high values of curvature ($|\nabla\cdot\mathbf{n}\delta_L| > 15$): this is associated to the relatively low number of points in this range of curvature within the flame brush and therefore are excluded from the representation. Curvature and flame displacement speed are negatively correlated with a strong variation across the flame brush and, flame elements with negative curvatures (curvature center in the unburnt mixture) propagate with faster flame speed than positively curved elements. Generally, the negative correlation of the total displacement speed S^*_d/S_L is stronger at negative curvatures and this asymmetry may be explained looking at the same asymmetric trend of the SDF $\sigma=|\nabla c|$ and at the dependence of S_d with $(|\nabla c|)^{-1}$. Comparing the displacement speeds of flames A and B in Fig. 3, it is observed that, when hydrogen is added (flame B), at c = 0.8, S_d is slightly smaller than flame negative curvature ($\nabla\cdot\mathbf{n}\delta_L<-2.5$) up to −20% at $\nabla\cdot\mathbf{n}\delta_L = -15$, while it is slightly greater for $\nabla\cdot\mathbf{n}\delta_L>-2.5$. This trend is governed by the reaction component S_r of the displacement speed.

Conclusions

Three-dimensional DNS of two turbulent premixed slot CH_4/H_2-Air flames has been carried out using detailed kinetics. Statistics such as average and rms fluctuations of streamwise and crosswise velocities, temperature and major species mass fraction are reported to characterize the flame and to define a new test case

for model validation purposes.
A progress variable, c, has been defined as sum of four species mass fractions: CO_2 $+CO+H_2O+H_2$. Each individual species has its own mass diffusion coefficient (modelled according to the Hirschfelder and Curtiss law). This differential diffusion is considered in deriving the expression for the displacement speed. Its individual contributions, like the reaction, normal and tangential terms, were analysed in details. The effects of differential diffusion are quantified based on the local equivalence ratio as a function of the progress variable curvature: a maximum difference of ∼3.7% in Φ is evidenced at the trailing edge of the flame A, when Soret effect is included (∼2.6% when no thermal diffusion is considered). For the enriched flame at 50% of H_2 the differential diffusion increases the variation of equivalence ratio up to 9%. The variation of equivalence ratio is mainly due to differential diffusivities of H_2 and O_2 , that result into higher differential diffusivity source terms. At the reaction zone, H_2 addition in flame B, reduces S^*/S_L, up to −20% at high negative curvature and increases it up to 30% for $\nabla\cdot\mathbf{n}\delta_L\sim$-15.

References

[1] S.A. Filatyev, J.F. Driscoll, C.D. Carter, J.M. Donbar, “Measured properties of turbulent premixed Flames for model assessment, including burning velocities, stretch rates, and surface densities”, *Combust. Flame*, 141, 1-21, (2005).

[2] E.S. Richardson, R. Sankaran, R.W. Grout, J.H. Chen, Numerical analysis of reaction-diffusion effects on species mixing rates in turbulent premixed methane-air combustion, Combust. Flame 157 (2012) 506-515.

[3] R. Sankaran, E.R. Hawkes, J.H. Chen, T. Lu, C.K. Law, Structure of a spatially developing turbulent lean methane-air Bunsen flame, Proc. Combust. Inst., 31, (2007) 1291-1298.

[4] J.C. Sutherland, P.J. Smith, J.H. Chen, Quantification of differential diffusion in non premixed systems, Combust. Theory Model. 9, (2005) 365-383.

doi: 10.4405/38proci2015.I3